ELSEVIER

Journal of Photochemistry and Photobiology A: Chemistry 144 (2001) 57–62

Journal of Photochemistry and Photobiology A:Chemistry

www.elsevier.com/locate/jphotochem

On the luminescence efficiency of polymer light-emitting diodes: a quantum-chemical investigation

D. Beljonne [a,*], Z. Shuai [a], J. Cornil [a], J.Ph. Calbert [a], J.L. Brédas [a,b]

[a] *Laboratory for Chemistry of Novel Materials, Center for Research on Molecular Electronics and Photonics, University of Mons-Hainaut, Place du Parc 20, B-7000 Mons, Belgium*

[b] *Department of Chemistry, The University of Arizona, Tucson, AZ 85721-0041, USA*

Abstract

Correlated quantum-chemical techniques are applied to the description of electronic excitations in luminescent conjugated polymers. We first address the role of intermolecular interactions on the emission properties of organic conjugated materials. The nature of the lowest excited states in molecular aggregates is discussed and a special emphasis is devoted to the chain-length dependence of the exciton coupling. By applying a molecular orbital perturbation approach, we then calculate the formation rates for singlet and triplet molecular excitons associated with intermolecular charge-transfer processes. Application of our approach to a model system for poly(paraphenylenevinylene) shows that the ratio between the electroluminescence and photoluminescence quantum yields generally exceeds the 25% spin-degeneracy statistical limit. © 2001 Elsevier Science B.V. All rights reserved.

Keywords: Poly(paraphenylenevinylene) (PPV); Light-emitting diodes (LED); Davydov splitting (DS)

1. Introduction

Since the discovery that a conjugated polymer, poly(paraphenylenevinylene) (PPV) can be used as the active component in light-emitting diodes (LED) [1,2], much effort has been devoted to the study of the luminescence properties of organic conjugated materials. These studies have largely contributed to the design of devices with performances that now compete with their inorganic counterparts. However, there is still a need for a fundamental understanding of the working mechanisms of polymer-based LEDs and the improvement of their characteristics. In this respect, quantum-chemical calculations can be useful by providing useful insight into the photophysics of conjugated materials.

For the achievement of highly efficient displays, the conjugated polymer has to fulfill a number of requirements, the most obvious one being to display high luminescence quantum yields in the solid state. Several strategies have been proposed in order to improve the electroluminescence (EL) quantum yields of organic conjugated polymers [3,4]. These aim at insuring: (1) a balanced injection for holes and electrons [5]; (2) an efficient electron-hole capture within the emissive layer (aided by using hole- and electron-transport materials in multilayer architectures [6]); (3) a strong radiative decay for the singlet excitons generated in the conjugated material (by control of microscopic order and sample purity [7]); and (4) an efficient coupling of the excitons to photon states allowed by the device structure (for instance, through the use of metallic mirrors [8,9]).

If up to now most of the theoretical investigations of the optical properties of organic conjugated polymers have been carried out on isolated chains, there is strong demand for the simulation of the corresponding properties in the solid state (films or crystals). This is motivated by an attempt to rationalize the generally observed decrease in luminescence quantum efficiency when going from solutions to films [10–13]. The lower emission quantum yield in the solid state is often ascribed to the presence of low-lying excited states with weak (or vanishing) radiative coupling to the ground state.

In the first part of this contribution (Section 2), we review the application of different formalisms (exciton theory and supermolecular approach) to the description of the lowest electronic excitations in interacting conjugated chains. We start with the simple case of dimers of stilbene and linear polyenes arranged in a face-to-face configuration [14]. We made this choice of systems in order to be able to discuss the evolution of the energy splitting associated with the $1B_u$ excited state, as a function of both interchain separation and conjugation length. We then investigate the evolution with oligomer size of the Davydov splitting in model clusters of oligothiophene single crystals [14].

---

[*] Corresponding author. Tel.: +32-65-37-3363; fax: +32-65-37-3366.

1010-6030/01/$ – see front matter © 2001 Elsevier Science B.V. All rights reserved.
PII: S1010-6030(01)00379-3

There exists a widely accepted perception that the EL efficiency is limited to 25% of that of photoluminescence (PL); this is based on simple spin statistics, namely, for the recombination of an electron and a hole (both with spin 1/2), there is a total of four micro-states: three triplet states and one singlet state. Very recendy, Cao et al. found that the ratio between EL and PL quantum efficiencies in a substituted PPV based LED can reach as high as 50% [15]. Since these authors attributed the 25% limit to be a consequence of the formation of strongly bound excitons, they conjectured that: (1) either the exciton binding energy is small; or (2) the cross-section for an electron-hole pair to form a singlet bound state is significantly higher than that to form a triplet [16]. Note, however, that in PPV the splitting between the lowest singlet and triplet excitons has been calculated to be on the order of 0.7 eV [17], which is large enough to inhibit any possible contribution from thermalized triplet excitons to luminescence [18]. We have thus considered case (2) [19] and show in Section 3 that the probability of forming a singlet or a triplet exciton can be different. In that case, the ratio η_2 between the number of optical singlet excitons and the total number of generated excitons has to be recast as $\eta_2 = \sigma_S/(\sigma_S + 3\sigma_T) = \sigma_{S/T}/(\sigma_{S/T} + 3)$, where $\sigma_{S(T)}$ is the cross-section for singlet (triplet) and $\sigma_{S/T} = \sigma_S/\sigma_T$. For $\sigma_S = \sigma_T$, we get $\eta_2 = 25\%$, the statistic limit; for $\sigma_S = 3\sigma_T$, $\eta_2 = 50\%$; for $\sigma_T = 0$, $\eta_2 = 100\%$.

2. Nature of the lowest excited states in conjugated chains aggregates

In traditional molecular exciton theory [20], the excited-state wavefunctions of the molecules in the aggregate (or crystal) are assumed to be unaffected by the intermolecular forces. Such an approximation is expected to be valid for weak (e.g. van der Waals-like) interactions. In this case, the spectroscopic properties of the cluster can be obtained through a first-order perturbation treatment, with the unperturbed isolated-chain wavefunctions as zero-order functions and the interchain Coulomb operator as the perturbation. Different approximations can be considered to solve this problem, such as the widely used dipole approximation. When applicable, molecular exciton theory allows the estimation of the energy splitting of the excited states responsible for the single-chain optical transitions, which arises because of the intermolecular interactions; it also provides useful information on the absorption cross-section (oscillator strength) and polarization of the electronic excitations appearing in the solid [20,21].

In the strong interaction limit, the excited states likely spread out over several molecules and a proper description of the electronic structure then requires building delocalized wavefunctions. This approach is known as the supermolecular approach, since it is then required to perform the calculation of the excited-state electronic structure by considering the ensemble of interacting conjugated chains as a single entity [22]. An important asset of this technique is that it inherently accounts for charge-transfer excitations among different chains, which is not the case in exciton theory, unless the basis set is augmented.

We have initially considered the ideal case of highly symmetric complexes by building cofacial dimers where two conjugated units are exactly superimposed on top of one another. The supermolecular wavefunctions were obtained by combining the INDO Hamiltonian [23] to a single configuration interaction (SCI) scheme. Fig. 1 displays the evolution of the lowest two optical transitions in cofacial dimers formed by two stilbene chains as the interchain distance goes from 20 down to 3.5 Å; these two optical features result from the interaction between the lowest optically-allowed $1B_u$ excited state of each chain. The theoretical results demonstrate that: (1) the lowest excited state of the dimer is not optically coupled to the ground state, whatever the interchain separation; and (2) the intensity is concentrated in the second excited state (or in a higher-lying state at short interchain distances, i.e. below 4 Å). This can be qualitatively understood on the basis of a dipole–dipole interaction model [20]: the lowest excited state then originates from a destructive interaction of the two intrachain transition dipole moments while the second excited state results from their constructive interaction; however, a simple point-dipole approximation provides reliable estimates for the optical splittings only when the interchain separation is larger than the size of the interacting units [20,24]. The calculations establish that the

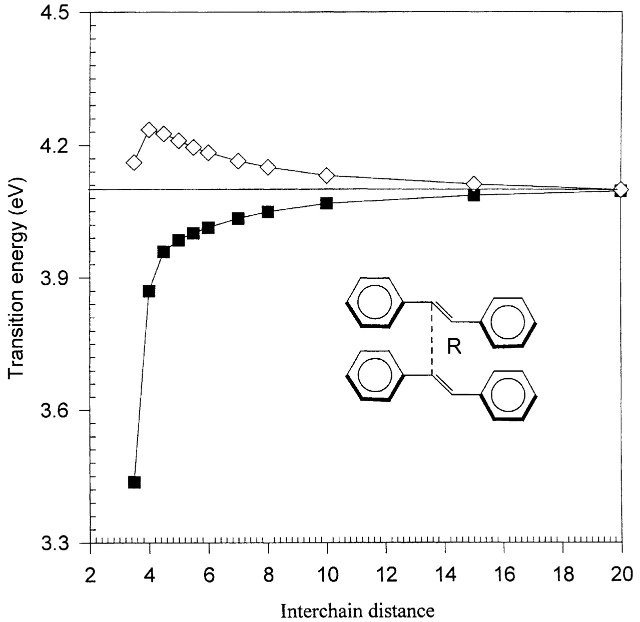

Fig. 1. Evolution of the INDO/SCI-calculated lowest two optical transitions in cofacial dimers constituted by two stilbene molecules as a function of the interchain distance, *R* (in Å). The horizontal line refers to the transition energy calculated for the $1B_u$ excited state of the isolated chain. We stress that the upper value reported at 3.5 Å actually corresponds to the fifth excited state of the dimer, which gives rise to the lowest intense absorption peak.

exciton splitting energy increases when the interchain distance is reduced. The splitting is symmetric with respect to the transition energy calculated for the isolated stilbene unit for large separations; this does not hold true at the strong interaction limit where charge-transfer contributions become significant.

It is also of interest to investigate the way the optical splitting calculated at fixed interchain distance evolves with the size of the interacting unit. We display in Fig. 2 the evolution of the exciton splitting in cofacial dimers formed by two polyenes separated by 6 Å, as a function of the inverse number of carbon atoms; here, the splittings are calculated with three different formalisms, namely: (1) the supermolecular approach; (2) the point-dipole approximation; and (3) an exciton model based on a multicentric monopole expansion of the electronic transition density, in which the splitting $W = 2|\beta|$ is estimated from the atomic transition densities associated to the lowest optically-allowed transition of a single chain [14].

Both the supermolecular approach and the exciton model based on atomic transition densities indicate that the exciton splitting passes by a maximum before asymptotically decreasing as the chains elongate [14]. In contrast, the point-dipole model yields largely overestimated exciton splittings and an inconsistent chain-length evolution since the splitting increases with N. These results cast strong doubt on any detailed interpretation of optical properties in molecular aggregates based on the point-dipole approximation.

The small differences between the values calculated within the other two approaches can be attributed to the neglect of the charge-transfer contributions in the excitonic model. Analysis of the chain-length evolution of the optical splittings reveals that the position of the maximum is shifted to longer chain lengths when the interchain separation is increased; the occurrence of such a peak behavior results from a subtle interplay between finite-size and delocalization effects [14]. The calculations thus suggest that luminescence quenching due to interchain effects is expected to get significantly reduced in well-ordered fully-conjugated long chains; this appears consistent with experimental data showing that concentration quenching, typically observed in dyes, can be absent in conjugated polymers [25].

We now turn to oligothiophenes. The magnitude of the exciton coupling energy in quaterthienyl (T_4) and sexithienyl (T_6) single crystals has been recently determined by means of polarized absorption measurements and quantum-chemical calculations based on the supermolecular approach [26,27]. In these crystals, the optically accessible Davydov components, a_u and b_u, are polarized along the b axis of the crystal and in the ac crystal plane, respectively. The energy difference between the one-photon allowed Davydov components (a_u and b_u crystal levels) gives the Davydov splitting of the corresponding exciton due to intermolecular interactions in the solid state.

Here, we apply the same supermolecular approach to the calculation of the Davydov splitting in single crystals of bithienyl (T_2) and octathienyl (T_8) [14]. Because of the layered 2-D character of the T_n crystals, we only consider clusters of molecules lying within the same bc layer to model the optical properties of the crystals. In Fig. 3, we show the evolution with cluster size of the Davydov splitting, as calculated by the INDO/SCI method in oligothiophenes with 2, 4, 6, and 8 aromatic rings. As is the case for sexithienyl [26], the Davydov splitting in T_2, T_4, and T_8 is found to evolve strongly with the number of

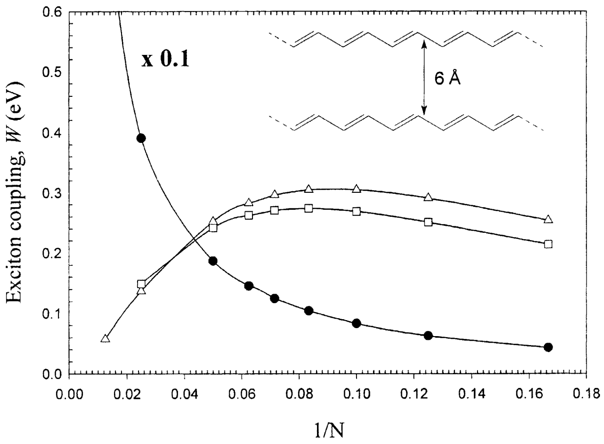

Fig. 2. Evolution of the exciton coupling energy in cofacial dimers formed by two polyene chains separated by 6 Å as a function of the inverse number of carbon atoms N, as estimated from: the supermolecular approach (open squares); the point-dipole approximation (filled circles); and the exciton model based on atomic transition densities (open triangles). The values obtained within the point-dipole model have been scaled by a factor of 0.1.

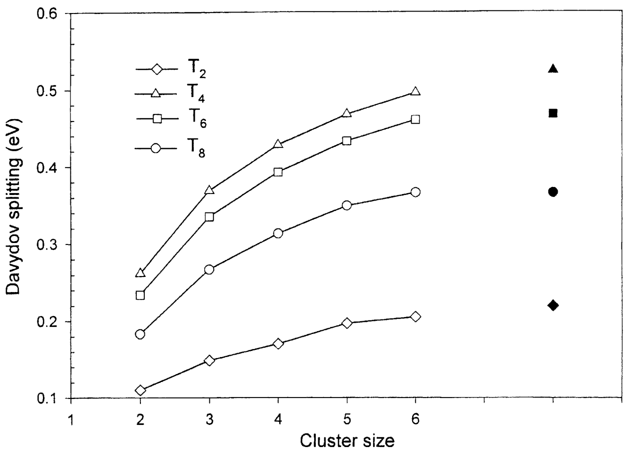

Fig. 3. INDO/SCI computed evolution of the Davydov splitting (in eV) in T_2 (open circles), T_4 (open squares), T_6 (open triangles), and T_8 (open diamonds) with the number of molecules in the clusters, as obtained on the basis of the supermolecular approach. The corresponding Davydov splittings estimated for an infinite cluster, when retaining only nearest neighbor interactions, are also indicated (closed symbols).

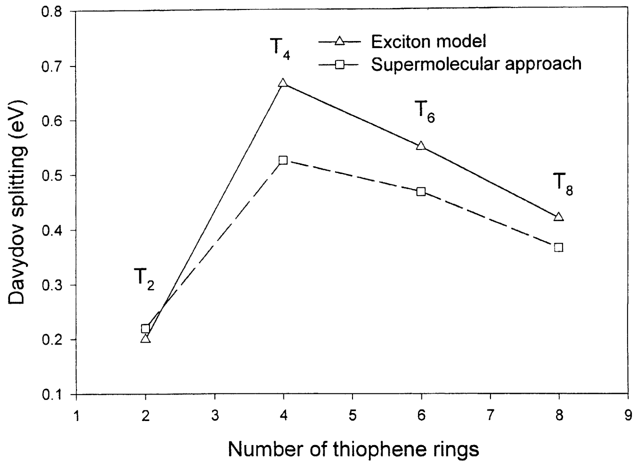

Fig. 4. Evolution with the number of thiophene aromatic rings in the conjugated chain of the Davydov splitting (in eV) in oligothiophene crystals (with only nearest neighbor interactions), as obtained: (i) on the basis of the exciton model and using the atomic transition densities (solid line, triangles); and (ii) on the basis of the supermolecular approach (dashed line, squares).

molecules in the clusters and to converge towards a saturated value for clusters containing about six conjugated chains. We can thus reasonably consider the excitation energies (and the corresponding Davydov splittings) calculated in the largest clusters investigated in this work, to be representative of the crystals. Furthermore, the splittings calculated in the six-chain clusters are close to twice the corresponding values in the two-chain clusters, which indicates that the dominant interactions are between nearest neighbors.

The evolutions with n of the Davydov splittings in the T_n crystals, as provided by both the supermolecular approach and the excitonic model, are reported in Fig. 4. The splittings reported here are set as twice the values calculated for the dimers (thus effectively applying a tight-binding approach). As found for cofacial polyenes, the results provided by the two methods are in good agreement and indicate a peak behavior for the chain-length dependence of the exciton coupling energy: the Davydov splitting (DS) first increases when going from T_2 to T_4, is maximum for T_4, and then decreases for longer conjugated segments.

Experimentally [26,27], the DS in oligothiophenes has been demonstrated to slightly decrease (by about 0.037 eV) when passing from T_4 (DS ~ 0.360 eV) to T_6 (DS ~ 0.323 eV), which is consistent with the predicted evolution in Fig. 4. In addition, the DS values computed for T_4 and T_6 are in reasonable agreement (although slightly overestimated) with the spectroscopic results, taken into account the different approximations considered in the calculations. In fact, we have shown in the case of T_6 that a better match between theory and experiment can be obtained by considering in the theoretical model the lattice relaxation taking place in the excited states [26].

3. Singlet and triplet formation cross-sections

In this section, we apply molecular orbital (MO) theory to a two-chain model to calculate the formation probabilities of singlet and triplet excitons from an electron and a hole localized on two adjacent chains [19]. The one-chain model Hamiltonian is the Pariser–Parr–Pople (PPP) Hamiltonian. We then apply the single configuration interaction (SCI) approach to calculate the intrachain exciton states. The spin-adapted exciton wavefunctions can be obtained from SCI as

$$|x1\rangle = \frac{1}{\sqrt{2}}\sum_{i_1 a_1} Z_{i_1 a_1}(a^{+}_{1\uparrow} i_{1\uparrow} \pm a^{+}_{1\downarrow} i_{1\downarrow})|\text{HF-SCF}\rangle \qquad (1)$$

where index ‘1’ indicates polymer chain 1; ‘+’ and ‘−’ represent singlet and triplet excited states, respectively. Z_{ia} is the CI coefficient (wavefunction) associated with an electronic configuration built by promoting one electron from occupied MO i to virtual MO a; $|\text{HF-SCF}\rangle$ denotes the Hartree–Fock self-consistent-field ground-state Slater determinant.

For a system consisting of two interacting chains, we can form two initial states to mimic the charge transport processes in EL devices:

$$|\text{in}_1\rangle = \frac{1}{\sqrt{2}}(L^{+}_{2\uparrow} H_{1\uparrow} \pm L^{+}_{2\downarrow} H_{1\downarrow})|\text{HF-SCF}\rangle;$$
$$|\text{in}_2\rangle = \frac{1}{\sqrt{2}}(L^{+}_{1\uparrow} H_{2\uparrow} \pm L^{+}_{1\downarrow} H_{2\downarrow})|\text{HF-SCF}\rangle \qquad (2)$$

with ‘+’ for singlet and ‘−’ for triplet. L_2 the LUMO (lowest unoccupied molecular orbital) of chain 2, and H_2 the HOMO (highest occupied molecular orbital) of chain 2, etc. Here, we assumed that the injected electron is located in the LUMO level of one conjugated chain and the hole in the HOMO level of the other chain; this is reasonable since the electron (hole) can relax from higher unoccupied (lower occupied) orbitals to the lowest (highest) one. Here, $|\text{in}_1\rangle$ $\{|\text{in}_2\rangle\}$ describes an initial state with an electron on chain 2 $\{1\}$ and a hole on chain 1 $\{2\}$. If we assume that the final exciton state takes the form expressed in Eq. (1), where chain 1 is the luminescence center, the processes starting from the two initial states of Eq. (2) correspond to electron transport (ET) and hole transport (HT), respectively.

The transition rates from the interchain electron-hole pair states (Eq. (2)) to the on-chain exciton (Eq. (1)) can be computed from the matrix elements $\langle x1|H'|\text{in}_1\rangle$ and $\langle x1|H'|\text{in}_2\rangle$, where H' is the interchain Hamiltonian containing both one- and two-electron terms. We found that both the interchain one-electron transfer matrix elements, $t^{\perp}$, and the two-electron bond-charge integrals, $X^{\perp}$, contribute to the description of the charge recombination process [19]. The $t^{\perp}$ terms correspond to the probability for an electron to jump from chain 1 to chain 2 and the $X^{\perp}$ terms represent the electron repulsion between the electron density around a bond on chain 1 and a site on chain 2. For simplicity, we assume an exponential dependence on distance for both $t^{\perp}$ and $X^{\perp}$: $e^{-\zeta r}$, ζ being fixed at 1.4 Å^{-1}, and we treat the ratio of $X^{\perp}/t^{\perp}$ as a variable.

We have considered two limiting cases [19]: (1) weak intermolecular coupling: the electronic states are localized on single chains; and (2) strong coupling: the electronic states are coherent combinations of localized states. The strength of coupling is relative to the energetic disorder: a strong disorder induces excitation localization [28]. In the first case, the on-chain excitation is given by Eq. (1), and the initial charge transfer states are expressed by Eq. (2). In the second case, there are two Davydov states:

$$|D_1\rangle = \frac{(|x1\rangle + |x2\rangle)}{\sqrt{2}}, \quad |D_2\rangle = \frac{(|x1\rangle - |x2\rangle)}{\sqrt{2}}$$

with $|x2\rangle$ for the exciton wavefunction localized on chain 2. The $|D_1\rangle$ state is optically allowed if the two chains are aligned parallel to each other, while $|D_2\rangle$ is dark ($|x1\rangle$ and $|x2\rangle$ are optically allowed themselves). Here, the initial charge pair states are no longer described by Eq. (2); they should be

$$|D_3\rangle = \frac{(|\mathrm{in}1\rangle + |\mathrm{in}2\rangle)}{\sqrt{2}} \quad \text{and} \quad |D_4\rangle = \frac{(|\mathrm{in}1\rangle - |\mathrm{in}2\rangle)}{\sqrt{2}}$$

In both limiting cases, numerical calculations were performed on two six-ring PPV oligomers interacting in a cofacial arrangement with an interchain distance of 4 Å. In Fig. 5, we depict the evolution of the singlet versus triplet cross-section ratio as a function of $X^{\perp}/t^{\perp}$ for the weak and strong coupling cases. For small X values, the singlet to triplet ratio is always around 1.27, which amounts to an η_2 value of 29.7%, *slightly larger* than the statistical limit of 25%. This is due to the difference in the CI coefficients for the singlet and triplet excitons, the contribution from the HOMO–LUMO excitation configuration being larger for the singlet exciton than for the triplet exciton. As a consequence, and this constitutes a crucial aspect, the wavefunction of the lowest singlet excited state resembles more that of the lowest charge-separated state, while the lowest triplet has a more confined character [17]: this is what leads to the larger cross-section with the singlet. Since usually $X^{\perp}/t^{\perp} \ll 0.8$, we expect in the case of weak coupling not much difference between the formation probabilities of singlet and triplet excitons and an η_2 of ~0.3.

In the case of full coherence, Fig. 5b, the two Davydov states have different behaviors as X is increasing. For the optically active state, $|D_1\rangle$, there occurs a resonance for $X^{\perp}/t^{\perp}$ ranging from 0.15 to 0.5 while for the optically forbidden state $|D_2\rangle$, the ratio is around unity for most of the $X^{\perp}/t^{\perp}$ values (with singlet slightly more favorable). In the experiments of Cao et al. [14], electron-transport materials are blended into PPV to insure balanced injections of holes and electrons. This is expected to improve the coherence between electrons and holes, so that the scenario associated with the limiting case of D_1 in Fig. 5b becomes applicable. In this case, a modest $X^{\perp}/t^{\perp} = 0.12$ gives $\sigma_{\mathrm{S/T}} = 3$, namely $\eta_2 =$ 50%. It is remarkable to note that a singlet-to-triplet exciton formation ratio largely exceeding the spin statistics limit has also been reported in a PPV derivative based LED, in which nearly quantitative balanced injection of charge carriers is achieved through molecular-scale engineering of the electrodes [16].

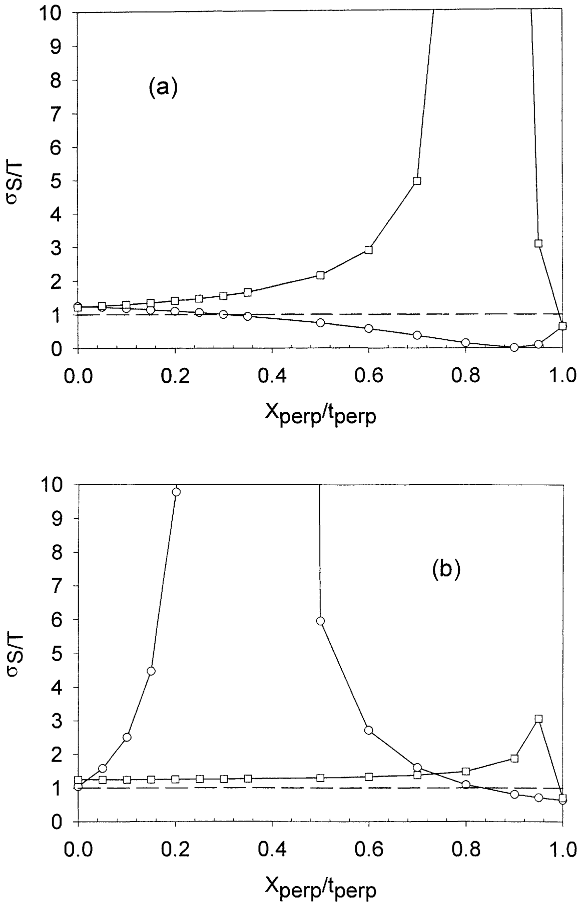

Fig. 5. Evolution of the ratio between singlet exciton and triplet exciton formation cross sections $\sigma_{\mathrm{S/T}}$ as a function of $X^{\perp}/t^{\perp}$: (a) in the case of weak coupling, circle for electron transport, square for hole transport; and (b) in the coherent case (Davydov states), circle for optically active $\mathrm{D_1}$ state, square for $\mathrm{D_2}$.

A feature omitted in this work is the consideration of the energy conservation factor, namely, the dissipation into the lattice of the binding energies of both singlet and triplet excitons. We note that in a variety of conjugated materials the triplet state lies 0.5–1.0 eV below the singlet exciton [29–31]; this fact thus is expected to further favor the formation of singlets over triplets.

4. Conclusions

In conclusion, we have illustrated that correlated quantum-chemical calculations performed on molecular aggregates can prove very helpful to rationalize the influence of interchain effects on the luminescence properties and to design strategies towards efficient light-emitting devices. Most importantly, we found that, in contrast to the point dipole excitonic model, calculations that properly account for the interchain interactions lead to a decrease of the exciton coupling with increasing conjugation length. The supermolecular approach can also give access to a detailed analysis of the one-electron structure of the clusters; this in turn can be used to gain a good theoretical insight into transport properties in crystalline materials on the basis of the calculated interchain transfer integrals [32].

We have calculated the formation cross section ratios of singlet with respect to triplet excitons in PPV through charge transfer processes. It is found that correlation effect of bond-charge type distinguishes singlet from triplet exciton formation rates. The correlation effect is found to be very much pronounced for the optically allowed Davydov exciton state, where even a very small bond-charge interaction can bring a large difference in singlet and triplet formation cross sections. The ratio between the electroluminescence and photoluminescence quantum efficiency yields is calculated to generally exceed the 25% spin-degeneracy statistical limit. We explain this result by the difference between the triplet and singlet exciton wavefunctions, the latter being more delocalized and therefore leading to a better overlap with the initial charge-separated excited state.

Overall, this study suggests the following strategies for the optimization of the performances of polymer-based LEDs:

1. design conjugated polymers that consist of highly extended conjugated chains with good interchain order, in such a way as to improve the charge transport within the organic films, while minimizing the luminescence quenching in the solid state;
2. tailor the charge injection barriers, through the use of appropriate electrode materials, in order to balance the electron and hole injections and boosts the singlet formation route with respect to the triplet route.

Acknowledgements

The work in Mons is partly supported by the Belgian Federal Services for Scientific, Technical, and Cultural Affairs (InterUniversity Attraction Pole, program PAl 4/11), the Belgian National Fund for Scientific Research (FNRS/FRFC), and the European Commission (BRITE-EURAM contract BRPR-CT97-0469 OSCA). J.C. and D.B. are research fellows of the Belgian National Fund for Scientific Research (FNRS). The work at the University of Arizona is supported in part by ONR through the MURI Center for Advanced Multiflinctional Polymers (CAMP).

References

[1] J.H. Burroughes, D.D.C. Bradley, A.R. Brown, R.N. Marks, K. Mackay, R.H. Friend, P.L. Burn, A.B. Holmes, Nature 347 (1990) 539.
[2] G. Gustafsson, Y. Cao, G.M. Treacy, F. Klavetter, N. Colaneri, A.J. Heeger, Nature 357 (1992) 477.
[3] R.H. Friend, R.W. Gymer, A.B. Holmes, J.H. Burroughes, R.N. Marks, C. Taliani, D.D.C. Bradley, D.A. dos Santos, M. Lögdlund, W.R. Salaneck, Nature 397 (1999) 121.
[4] J.R. Sheats, H. Antoniadis, M. Hueschen, W. Leonard, J. Miller, R. Moon, D. Roitman, A. Stocking, Science 273 (1996) 884.
[5] I.D. Parker, J. Appl. Phys. 75 (1994) 1656.
[6] N.C. Greenham, S.C. Moratti, D.D.C. Bradley, R.H. Friend, A.B. Holmes, Nature 365 (1993) 628.
[7] S. Son, A. Dodabalapur, A.J. Lovinger, M.E. Galvin, Science 269 (1995) 376.
[8] H. Becker, S.E. Bums, R.H. Friend, Phys. Rev. B 56 (1997) 1893.
[9] N. Tessler, Adv. Mater. 11 (1999) 363.
[10] M. Yan, L.J. Rothberg, E.K. Kwock, T.M. Miller, Phys. Rev. Lett. 75 (1995) 1992.
[11] L.J. Rothberg, M. Yan, F. Papadimitrakopoulos, M.E. Galvin, E.K. Kwock, T.M. Miller, Synth. Met. 80 (1996) 41.
[12] I.D.W. Samuel, G. Rumbles, R.H. Friend, in: N.S. Sariciftci (Ed.), Primary Photoexcitations in Conjugated Polymers, World Scientific, Singapore, 1997, p. 140.
[13] D. Oelkrug, H.-J. Hegelhaaf, D.R. Worrall, F. Wilkinson, J. Fluoresc. 5 (1995) 165.
[14] D. Beljonne, J. Cornil, J.L. Bredas, P. Millié, R. Silbey, J. Chem. Phys. 112 (2000) 4749.
[15] Y. Cao, I.D. Parker, G. Yu, C. Zhang, A.J. Heeger, Nature 397 (1999) 414.
[16] P.K.H. Ho, J.-S. Kim, J.H. Burroughes, H. Becker, S.F.Y. Li, T.M. Brown, F. Cacialli, R.H. Friend, Nature 404 (2000) 481.
[17] D. Beljonne, Z. Shuai, R.H. Friend, J.L. Brédas, J. Chem. Phys. 102 (1995) 2042.
[18] A.L. Burin, M.A. Ratner, J. Chem. Phys. 102 (1998) 6092.
[19] Z. Shuai, D. Beljonne, R.J. Silbey, J.L. Bredas, Phys. Rev. Lett. 84 (2000) 131.
[20] M. Pope, C.E. Swenberg, Electronic Processes in Organic Crystals, Oxford University Press, New York, 1982.
[21] M. Kasha, Radiation Res. 20 (1963) 55.
[22] J. Cornil, D.A. dos Santos, X. Crispin, R. Silbey, J.L. Brédas, J. Am. Chem. Soc. 120 (1998) 1289.
[23] J. Ridley, M.C. Zemer, Theor. Chim. Acta 32 (1973) 111.
[24] Z.G. Soos, G.W. Hayden, P.C.M. McWilliams, S. Etemad, J. Chem. Phys. 93 (1990) 7439.
[25] F. Hide, M.A. Diaz-Garcia, B.J. Schwartz, A.J. Heeger, Acc. Chem. Res. 30 (1997) 430.
[26] M. Muccini, E. Lunedei, C. Taliani, D. Beljonne, J. Cornil, J.L. Brédas, J. Chem. Phys. 109 (1998) 10513.
[27] M. Muccini, M. Schneider, C. Taliani, M. Sokolowski, E. Umbach, D. Beljonne, J. Comil, J.L. Brédas, Phys. Rev. B 62 (2000) 6296.
[28] M.J. Rice, Yu.N. Gartstein, Phys. Rev. B 53 (1996) 10764.
[29] J. Seixas de Melo, L.M. Silva, L.G. Arnaut, R.S. Becker, J. Chem. Phys. 111 (1999) 5427.
[30] R. Osterbacka, M. Wohlgenannt, Z.V. Vardeny, Phys. Rev. B 60 (1999) 1253.
[31] Y. Romanovskii, A. Fischer, U. Scherf, R. Personov, H. Bässler, Phys. Rev. Lett. 84 (2000) 1027.
[32] J. Comil, J.Ph. Calbert, D. Beljonne, J.L. Bredas, Adv. Mater. 12 (2000) 978.